Craig H and Gordon LI (1965) Deuterium and oxygen-18 variations in the oceans and marine atmosphere. In: Tongiorgi E (ed.) *Stable Isotopes in Oceanographic Studies and Paleotemperatures*, pp. 1–122. Spoleto: Consiglio Nazionale delle Ricerche, Laboratorio di Geologica Nucleare, Pisa.

Emiliani C (1955) Pleistocene temperatures. *Journal of Geology* 63: 539–578.

Epstein S, Buchsbaum R, Lowenstam H and Urey HC (1953) Revised carbonate-water temperature scale. *Bulletin of the Geological Society of America* 64: 1315–1326.

Fairbanks RG, Charles CD and Wright JD (1992) Origin of Melt Water Pulses. In: Taylor RE, Long A and Kra RS (eds) *Radiocarbon After Four Decades*, pp. 473–500. New York: Springer-Verlag.

Imbrie J, Hays JD, Martinson DG *et al.* (1984) The orbital theory of Pleistocene climate: support from a revised chronology of the marine $\delta^{18}O$ record. In: Berger AL, Imbrie J, Hays JD, Kukla G and Saltzman B (eds) *Milankovitch and Climate*, part I, pp. 269–305. Dordrecht: Reidel.

Lear CH, Elderfield H and Wilson PA (1999) Cenozoic deep-sea temperatures and global ice volumes from Mg/Ca in benthic foraminiferal calcite. *Science* 287: 269–272.

Miller KG, Fairbanks RG and Mountain GS (1987) Tertiary oxygen isotope synthesis, sea-level history, and continental margin erosion. *Paleoceanography* 2, 1–19.

Miller KG, Wright JD and Fairbanks RG (1991) Unlocking the Ice House: Oligocene–Miocene oxygen isotopes, eustasy, and margin erosion. *Journal of Geophysical Research* 96: 6829–6848.

Pagani M, Arthur MA and Freeman KH (1999) Miocene evolution of atmospheric carbon dioxide. *Paleoceanography* 14: 273–292.

Palmer MR, Pearson PN and Cobb SJ (1998) Reconstructing past ocean pH-depth profiles. *Science* 282: 1468–1471.

Pearson PN and Palmer MR (1999) Middle Eocene seawater pH and atmospheric carbon dioxide concentrations. *Science* 284: 1824–1826.

Rozanski K, Araguas-Araguas L and Gonfiantini R (1993) Isotopic patterns in modern global precipitation. In: Swart PK, McKenzie J and Savin S (eds) *Climate Change in Continental Isotopic Records*. Geophysical Monograph 78, pp. 1–35. Washington, DC: American Geophysical Union.

Rye DM and Sommer MA (1980) Reconstructing paleotemperature and paleosalinity regimes with oxygen isotopes. In: Rhoads DC and Lutz RA (eds) *Skeletal Growth of Aquatic Organisms*, pp. 162–202. New York: Plenum.

Savin SM, Douglas RG and Stehli FG (1975) Tertiary marine paleotemperatures. *Geological Society of America Bulletin* 86: 1499–1510.

Shackleton NJ (1967) Oxygen isotope analyses and Pleistocene temperatures re-assessed. *Nature* 215: 115–117.

Shackleton NJ, Berger A and Peltier WR (1990) An alternative astronomical calibration of the Lower Pleistocene time scale based on ODP Site 677. *Transactions of the Royal Society of Edinburgh*, *Earth Science* 81: 251–261.

Shackleton NJ and Kennett JP (1975) Paleotemperature history of the Cenozoic and initiation of Antarctic glaciation. Oxygen and carbon isotopic analysis in DSDP Sites 277, 279, and 281. *Initial Report. Deep Sea Drilling Project* 29, 743–755.

Shackleton NJ and Opdyke ND (1973) Oxygen isotope and paleomagnetic stratigraphy of equatorial Pacific core V28-238. Oxygen isotope temperatures and ice volumes on a 10^5 year and 10^6 year scale. *Quaternary Research* 3: 39–55.

Tiedemann RM, Sarnthein M and Shackleton NJ (1994) Astronomic calibration for the Pliocene Atlantic $\delta^{18}O$ and dust flux records of Ocean Drilling Program Site 659. *Paleoceanography* 9: 619–638.

Urey HC (1947) The thermodynamic properties of isotopic substances. *Journal of the Chemical Society* pp. 562–581.

CENOZOIC OCEANS – CARBON CYCLE MODELS

L. François and Y. Goddéris, University of Liège, Liège, Belgium

doi:10.1006/rwos.2001.0253

Introduction

The story of the Cenozoic is essentially a story of global cooling. The last 65 million years of the Earth's history mark the transition from the Cretaceous 'greenhouse' climate toward the present-day 'icehouse' conditions. Particularly, the cooling by about 8–10°C of deep ocean waters since the Cretaceous was linked to a reorganization of the oceanic circulation triggered by tectonic plate movements. These oceanic circulation changes were coeval with continental climatic change, as demonstrated by abundant evidence for global cooling (pollen, faunal assemblages, development of glaciers, etc.). For instance, most of western Europe and the western United States had a subtropical climate during the Eocene, despite the fact that they were located at

the same latitude as today. Another striking feature of the changes that have occurred during Cenozoic times is the decrease of the partial pressure of atmospheric CO_2 (P_{CO_2}). Since CO_2 is a greenhouse gas, there might be a causal relationship between the decrease in P_{CO_2} and the general cooling trend of Cenozoic climate. The global cooling might be the result of the changes in oceanic circulation and atmospheric CO_2, both probably influencing each other and possibly initiated by tectonic processes.

Indicators of Atmospheric CO_2 Change

It should be kept in mind that there are no direct proxies of ancient levels of CO_2 in the atmosphere. Methods rely on three indirect indicators.

1. The $\delta^{13}C$ measured in ancient soil carbonates can be directly linked to the atmospheric P_{CO_2}. This method reveals declining atmospheric P_{CO_2} over the last 65 million years, from about 650 ppm by volume (ppmv) in the Paleocene (**Figure 1**).
2. The biological isotopic fractionation occurring during assimilation of carbon by the marine biosphere (ε_p) depends on the partial pressure of CO_2 dissolved in sea water, itself directly related to the atmospheric P_{CO_2}. The estimation of ε_p for ancient organic sediments indicates high P_{CO_2} values in the Eocene (620 ppmv), followed by a constant decline toward the present-day pressure through the Cenozoic (**Figure 1**).
3. The measured boron isotopic composition of marine carbonates gives insight into the pH of ancient sea water. Assuming a plausible history for the ocean alkalinity, lower or higher pH values can be respectively related to higher or lower P_{CO_2}. This method has been applied to the last 60 million years, showing values as high as 3500 ppmv CO_2 during the Paleocene. The decline in P_{CO_2} was then roughly linear through time until the late Eocene. During the last 25 million years of the Earth's history, P_{CO_2} was relatively constant, possibly displaying lower values than present-day ones during Miocene. No data are available for the Oligocene (**Figure 1**).

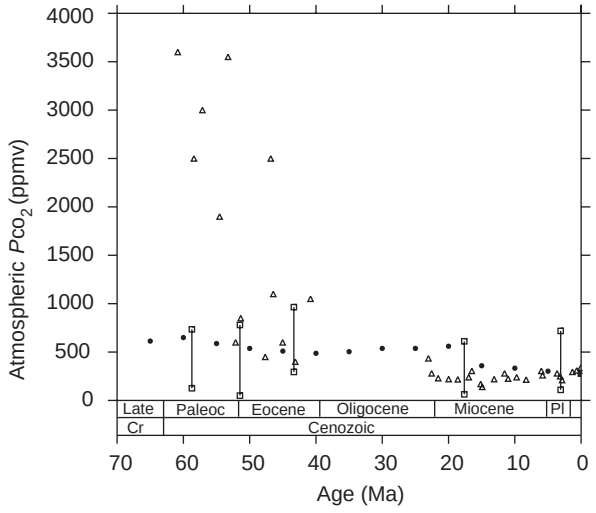

Figure 1 The reconstructed partial pressure of atmospheric CO_2. Δ, from boron isotopes (Pearson and Palmer, 2000) ; ●, from ε_p (Kump and Arthur, 1997); □, from paleosoils analysis (compilation by Berner, 1998). Timescale according to Harland *et al.* (1990) (CR = Cretaceous; PALEOC = Paleocene; PL = Pleistocene.)

Despite some disagreements between the three reconstructions, they all indicate a major reduction of the atmospheric CO_2 partial pressure during the Cenozoic, which might potentially play an important role in the coeval global cooling. Any exploration of the cause of the decline in P_{CO_2} requires the identification of the sources and sinks of oceanic and atmospheric carbon, and some knowledge of their relative changes during the Cenozoic.

Carbon Cycle Changes and Processes Involved

Long-term Regulation of Atmospheric CO_2

On the geological timescale, and neglecting at this point the possible impact of sedimentary organic carbon cycling, the sources of carbon for the ocean–atmosphere system are the degassing of the mantle and metamorphic processes. Carbon is injected as CO_2 into the ocean–atmosphere system today through the degassing of fresh basalts along mid-oceanic ridges (MOR) ($1.5–2.2 \times 10^{12}$ mol y^{-1}), and through plume events and arc volcanism ($1.5–5.5 \times 10^{12}$ mol y^{-1}). These various sources account for the total degassing flux F_{VOL}. Once released, this carbon is rapidly (within 10^3 years) redistributed between the atmosphere and the ocean, reaching a steady-state repartition after a negligible time compared to the geological timescale. Carbon can leave the system mainly through the deposition of carbonate minerals on the seafloor. The rate of carbon removal through carbonate deposition is controlled by the saturation state of the

ocean, and thus by the rate of supply of alkalinity by the chemical weathering of continental minerals. Carbonate and silicate minerals exposed at the continental surface weather under the corrosive action of atmospheric CO_2 dissolved in rain water as carbonic acid, and eventually concentrated by the microbial respiration in soils. Regarding the chemical weathering of carbonate minerals, the net budget of the dissolution reaction can be written as follows eqn [I].

$$CaCO_3\ (\text{rock}) + H_2CO_3\ (\text{atmosphere}) \rightarrow Ca^{2+}\ (\text{rivers}) + 2HCO_3^-\ (\text{rivers}) \quad [\text{I}]$$

In this reaction, there is a net transfer of Ca^{2+} (or Mg^{2+} in the case of magnesium carbonates) from the continental crust to the ocean, a creation of two equivalents of alkalinity and a transfer to the river system of two moles of carbon per mole of Ca^{2+}, one coming from the crust, the other one from the atmosphere. Once the weathering products reach the ocean, they will increase the saturation state of surface waters with respect to calcite and induce rapidly (within 10^3 years) the biologically driven precipitation of one mole of $CaCO_3$ followed by its deposition on the seafloor. The precipitation–deposition reaction is the reverse of reaction [1]. The net carbon budget of the weathering of carbonate minerals followed by deposition of sedimentary carbonate is thus equal to zero.

The chemical weathering of continental silicate rocks is fundamentally different, since silicate rocks do not contain carbon. The budget can be written as eqn [II].

$$CaSiO_3\ (\text{rock}) + 2\,H_2CO_3\ (\text{atmosphere}) + H_2O \rightarrow Ca^{2+}\ (\text{rivers}) + 2\,HCO_3^-\ (\text{rivers}) + H_4SiO_4\ (\text{rivers}) \quad [\text{II}]$$

Here $CaSiO_3$ stands for a 'generic' silicate mineral. The weathering reaction of more realistic Ca- (or Mg-) silicate minerals, if more complex, displays the same budget in terms of alkalinity versus carbon fluxes. Again, once reaching the ocean, the excess Ca^{2+} will precipitate as $CaCO_3$, thus removing one mole of carbon from the ocean per mole of weathered silicates. The net budget of this reaction, after sedimentary carbonate precipitation, is the transfer of exospheric carbon to the crust. Chemical weathering of continental silicate minerals thus acts as the main sink of carbon on the geological timescale. Today, about $6 \times 10^{12}\,\text{mol}\,\text{y}^{-1}$ of Ca^{2+} and Mg^{2+} are released from silicate weathering.

The size of the exospheric carbon pool (ocean + atmosphere) is about 3.2×10^{18} mol today. As mentioned above, the fluxes entering and leaving this reservoir are of the order of 10^{12}–$10^{13}\,\text{mol}\,\text{y}^{-1}$. A relatively small imbalance between the input and output of carbon of $10^{12}\,\text{mol}\,\text{y}^{-1}$, the output being higher, but persisting for several million years, will result in a drastic reduction in the exospheric content. Three million years will be sufficient to remove all the carbon from the exospheric system, thus forcing the atmospheric P_{CO_2} to zero. There is no lithological, fossil, or geochemical record of such a dramatic event during the Cenozoic, or event during the complete Phanerozoic. To avoid the occurrence of such events for which there is no evidence, the perturbations of the carbon cycle had to be limited in time and amplitude, and thus the past exospheric carbon cycle was not strictly at, but always close to, steady state. The same considerations apply to the alkalinity budget. These steady-state conditions require that the amount of carbon removed from the atmosphere–ocean system by continental silicate weathering must always closely track the amount of carbon released by degassing. Mathematically, these conditions translate into eqn [1].

$$F_{SW} = F_{VOL} \quad [1]$$

The question is now how to physically force F_{SW} to follow the degassing. The answer lies in the fact that the chemical weathering of continental silicates appears to be dependent on air temperature, the dissolution being enhanced during warmer climates. This dependence provides a negative feedback that not only allows equilibration of the carbon and alkalinity budgets on the geological timescale, but also stabilizes the Earth's climate. When the degassing increases suddenly, for instance as a result of a higher spreading rate of the oceanic floor, the amount of carbon in the ocean and atmosphere will first increase, increasing the atmospheric P_{CO_2}. Because CO_2 is a greenhouse gas, the climate will become warmer, and this will enhance the weathering of silicate rocks. As a result, any increase in the input of carbon will be counterbalanced by an increase of the output through silicate weathering, thus stabilizing the system through a negative feedback loop. The P_{CO_2} will stabilize at a somewhat higher level than before the perturbation. Similarly, the decline in P_{CO_2} through the Cenozoic could be due to a decreasing degassing rate, which acts as the driving force of changes. This simple process is the

basis of all existing long-term geochemical cycle models. It was first identified in 1981 by Walker, Hays, and Kasting. Breaking this feedback loop would result in fluctuations in calculated P_{CO_2} and thus presumably in climate, that are not reflected in the geological record.

Himalayan Uplift, $^{87}Sr/^{86}Sr$ Record and Possible Implications for Weathering History

M.E. Raymo in 1991 put forward another explanation of the global Cenozoic P_{CO_2} decline. Instead of a decreased degassing rate, she suggested that continental silicate weathering rates increased drastically over the last 40 million years, although degassing conditions remained more or less constant. This assertion was originally based on the Cenozoic carbonate record of $^{87}Sr/^{86}Sr$. The isotope ^{86}Sr is stable, whereas ^{87}Sr is produced by the radioactive β-decay of ^{87}Rb. Strontium ions easily replace calcium ions in mineral lattices, since their ionic diameters are comparable. The present-day sea water $^{87}Sr/^{86}Sr$ equals 0.709. Two main processes impinge on this ratio: the chemical weathering of continents, delivering strontium with a mean $^{87}Sr/^{86}Sr$ of 0.712, and the exchanges between seafloor basalts and sea water, resulting in the release of mantle strontium into the ocean ($^{87}Sr/^{86}Sr = 0.703$). In other words, chemical weathering of continental rocks tends to increase the strontium isotopic ratio of sea water, while exchanges with seafloor basalts at low or high temperature tend to decrease it.

The sea water $^{87}Sr/^{86}Sr$ recorded over the last 65 million years displays a major increase, starting about 37–38 million years ago (**Figure 2**). An event approximately coeval with the sea water $^{87}Sr/^{86}Sr$ upward shift is the Himalayan uplift, which was initiated by the India–Asia collision some 50 million years ago. Raymo has proposed that, in an uplifted area, the mechanical breakdown of rocks increases owing to the cooling and development of glaciers, to the development of steep slopes, and to temperatures oscillating below and above the freezing point at high altitudes. Furthermore, the development of the monsoon regime, about 10 million years ago, resulted in increased runoff, and thus an enhanced water availability for weathering, over at least the southern side of the Himalayan range. All these uplift-related changes might result in an enhanced chemical dissolution of minerals, since the surface in contact with the corrosive solutions increases when rocks fragment. The consequence of the Himalayan uplift might thus be an increase in the consumption of exospheric carbon by enhanced weathering on the continents, a process recorded in the sea water $^{87}Sr/^{86}Sr$ rise. The system depicted in this hypothesis is new, compared to the hypothesis described in the previous section. Here, tectonic processes result in uplift, followed by enhanced weathering, itself consuming atmospheric CO_2, thus cooling the climate. This cooling favors the development of glaciers not only in the uplifted area, but also globally, producing a global increase in mechanical and subsequent chemical weathering, a positive feedback that further cools the Earth. In Raymo's hypothesis, the negative feedback proposed by Walker *et al.*, stabilizing P_{CO_2} no longer exists. Chemical weathering is mainly controlled by tectonic processes with high rates in a cool world (Raymo's world), while it was controlled by climate and P_{CO_2} with high rates in a warm world in the Walker hypothesis (Walker's world). However, as mentioned above, negative feedbacks are needed to stabilize P_{CO_2}, especially since the degassing remained more or less constant over the period of interest. Raymo's world has the ability to exhaust atmospheric CO_2 within a few million years.

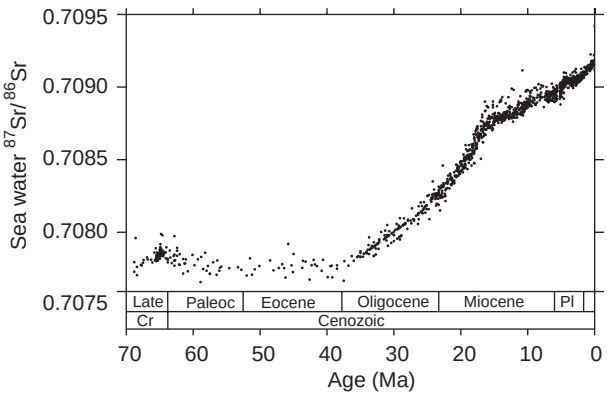

Figure 2 Sea water $^{87}Sr/^{86}Sr$ recorded in ancient carbonate sediments (Ottawa-Bochum database: http://www.science.uottawa.ca/geology/isotope_data/). Timescale abbreviations as **Figure 1**.

In an attempt to reconcile the two approaches, François and Walker proposed in 1992 the addition of a new CO_2 consumption flux to the carbon cycle, identified as the precipitation of abiotic carbonates within the oceanic crust, subsequent to its alteration at low temperature. This flux is directly dependent on deep water temperature, which has decreased by $\sim 8^{\circ}C$ over the Cenozoic. An increase in the continental weathering rate might be compatible with a constant degassing rate, since the sink of carbon through low-temperature alteration of the oceanic crust is decreasing. The balance between input and output is thus still in place. However, this additional

sink of carbon is poorly constrained. The present-day consumption of carbon is estimated to be about $1.4 \times 10^{12}\,\mathrm{mol\,y^{-1}}$, but the kinetics of the process is essentially unknown. This attractive hypothesis still needs experimental verification.

Finally, it should be noted that Raymo's hypothesis interprets the increase in the sea water $^{87}Sr/^{86}Sr$ in terms of an increase in the weathering fluxes. However, silicate minerals exposed in the Himalayan area, particularly in the High Himalayan Crystalline Series, display unusually high isotopic ratios (reaching 0.740). Sediments of Proterozoic age with a $^{87}Sr/^{86}Sr$ reaching 0.8 are also exposed in the Lesser Himalaya area. For this reason, rivers draining the Himalayan area (Ganges, Brahmapoutra, etc.) display an isotopic ratio (0.725 for the Ganges) higher than the mean global value (0.712). At least part of the Cenozoic increase in the sea water $^{87}Sr/^{86}Sr$ might thus be due to changes in the isotopic composition of source rocks.

Lysocline and Carbonate Accumulation Changes

Other indicators of a possible increase in the continental weathering rate over the course of Cenozoic exist. For instance, the global mean Calcite Compensation Depth (CCD) sank by about 1 km over the last 40 million years (**Figure 3**), a change possibly linked to an increased supply of alkalinity from rivers caused by the Himalayan uplift. Paradoxically, there is no evidence of major changes in the carbonate accumulation flux during the Cenozoic (**Figure 4**). The deepening of the CCD might thus be linked, at least partially, to the global Cenozoic marine regression, reducing the area of shallow epicontinental seas and thus the area available for the accumulation of coral reefs. In that case, carbon and alkalinity will be preferentially removed from the ocean through enhanced formation of calcitic shells in open waters, leading to the deepening of the CCD. This process might have been favored by the coeval development of new foraminiferal species. The cause of the CCD deepening thus remains unresolved.

Organic Carbon Subcycle

The Cenozoic history of sea water $\delta^{13}C$ recorded in marine limestones (**Figure 5**) is marked by an ample fluctuation in the Paleocene and early Eocene, a roughly constant background value with super-

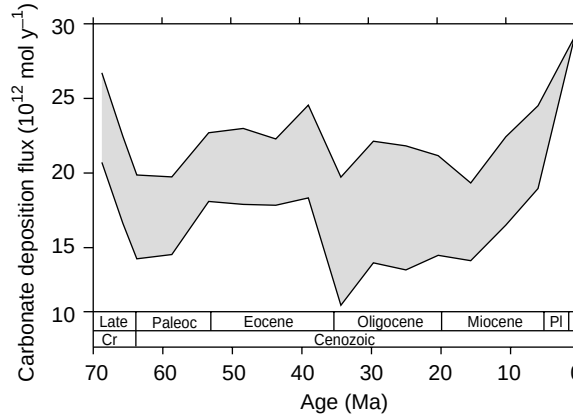

Figure 4 Total carbonate accumulation flux reconstructed from paleodata (Opdyke and Wilkinson, 1988). Timescale as **Figure 1**.

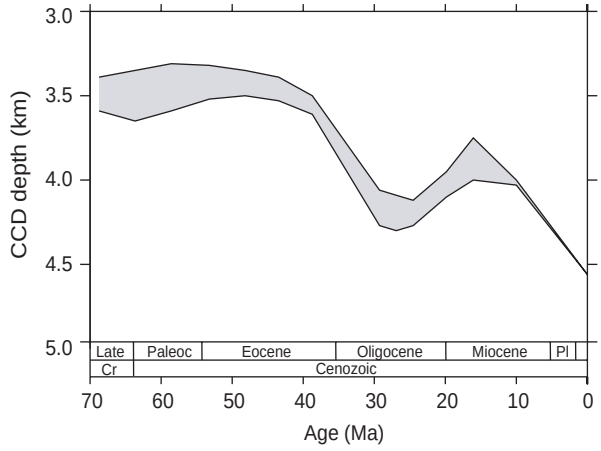

Figure 3 Reconstructed Carbonate Compensation Depth (CCD) through the Cenozoic (Van Andel, 1975; Broecker and Peng, 1982). Timescale as **Figure 1**.

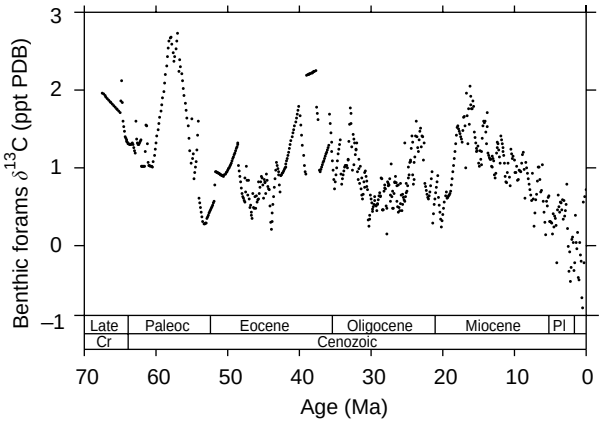

Figure 5 Sea water $\delta^{13}C$ recorded in ancient carbonate sediments (Ottawa-Bochum database: http://www.science.uottawa.ca/geology/isotope_data/). Timescale as **Figure 1**. ppt PDB = parts per thousand PeeDee Belemnite.

imposed high-frequency variations from the middle Eocene to the middle Miocene, and a sharp decrease from the middle Miocene to the present. Since organic matter is enriched in the lighter ^{12}C isotope with respect to sea water (owing to photosynthetic fractionation), this $\delta^{13}C$ record can be used to constrain the temporal changes in the organic fluxes of the carbon cycle. The burial of organic matter on the sea floor preferentially removes ^{12}C from the ocean and hence tends to increase seawater $\delta^{13}C$. Conversely, the oxidation of old organic carbon (kerogen) contained in weathered sedimentary rocks is a source of isotopically light carbon for the ocean, tending to decrease its $\delta^{13}C$. The recent decrease in $\delta^{13}C$ since mid-Miocene times might thus be interpreted as the result of kerogen carbon oxidation being larger than organic carbon burial during that period. Similarly, the overall constancy of sea water $\delta^{13}C$ from the middle Eocene to the middle Miocene may suggest that the organic subcycle was essentially balanced at that time. However, the average carbon isotopic fractionation (ε_{TOC}) between total organic carbon and sedimentary carbonate (which is close to coeval sea water) has decreased from the Eocene to the present (**Figure 6**). With a balanced organic subcycle, this change in ε_{TOC} would imply a decrease of the sea water $\delta^{13}C$ over time, as it forces the $\delta^{13}C$ of organic deposits to become closer to the sea water value than it is for kerogen carbon. For the isotopic composition of the ocean to remain constant from the middle Eocene to the middle Miocene, the trend associated with ε_{TOC} variations must be compensated for by an imbalance in the organic subcycle in which the burial of organic carbon exceeds kerogen oxidation. This imbalance was progressively reduced after mid-Miocene times, but may have persisted until very recently.

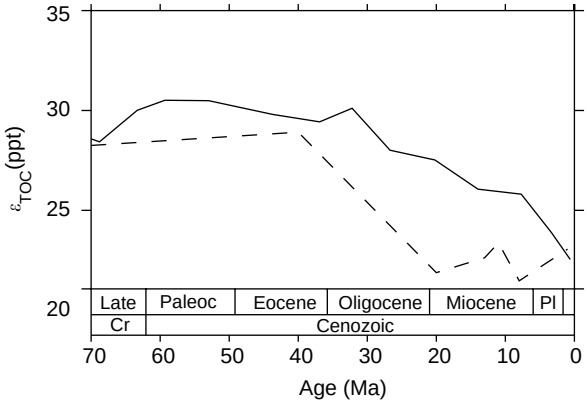

Figure 6 Average carbon isotopic fractionation (ε_{TOC}) between total organic carbon and sedimentary carbonate (solid line, Hayes *et al.* (1999); dashed line, Freeman and Hayes (1992)). Timescale as **Figure 1**.

The late Cenozoic was therefore a time of unusually high organic carbon deposition rates, leading to an increase in the size of the sedimentary organic carbon reservoir. The organic subcycle thus acted as a carbon sink over the course of the Himalayan uplift. There are two possible causes of this evolution.

1. The increase in chemical weathering rates in the Himalayan region during the uplift (Raymo's world) leads to enhanced delivery of nutrients to the ocean, forcing the oceanic primary productivity to increase. This might result in an increased burial of organic matter.
2. Enhanced mechanical weathering in the Himalayan region increased the sedimentation rate on the ocean floor, so that organic carbon was more easily preserved. This hypothesis does not require any increase in the chemical weathering rate in the Himalayan region. This facilitated burial might have significantly contributed to the Cenozoic P_{CO_2} decrease, since carbon is stored in a sedimentary reservoir. C. France-Lanord and L. Derry argued in 1997 that the consumption of CO_2 through organic carbon burial might be three times more important today than the amount of CO_2 consumed by silicate weathering within the orogen. Even if this hypothesis still links the climatic cooling with the Himalayan uplift, the origin of the CO_2 sink is quite different from that hypothesized in Raymo's world.

Observational data argue toward the second hypothesis, indicating that the Cenozoic increase in the sea water $^{87}Sr/^{86}Sr$ might be of isotopic origin. Calcium silicates are indeed not the most common mineral exposed in the Himalayan orogen, and thus cannot contribute widely to the CO_2 consumption. Furthermore, reverse weathering reactions take place in the Bengal Fan, releasing CO_2 and thus reducing the impact of the Himalayan silicate weathering on P_{CO_2}.

It has been suggested that the emission at some time in the past of large amounts of methane from gas hydrates may have influenced the $\delta^{13}C$ of the ocean. This may invalidate the interpretation of the carbon isotopic record if the gas hydrate reservoir has had long-term as well as shorter-term effects.

Organic carbon deposition on the seafloor is linked to ocean biological productivity, itself depending on the availability of nutrients, among which phosphorus is thought to play a key role. The

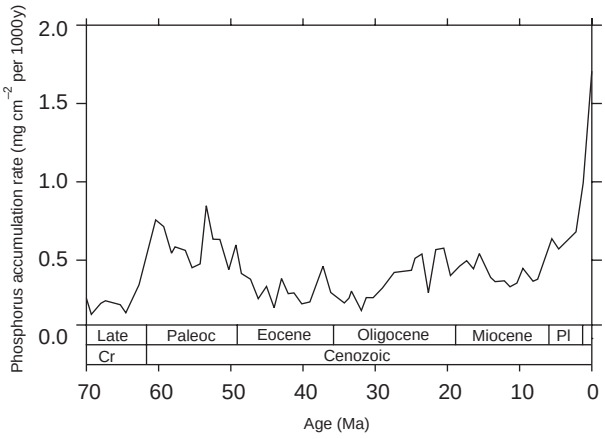

Figure 7 Average accumulation of phosphorus in sediments through the Cenozoic (Föllmi, 1995). Timescale as **Figure 1**.

global phosphorus accumulation into sediments increased by a factor of about 4 over the last 10 million years (**Figure 7**), interpreted as the record of a global continental weathering enhanced by the onset of large ice sheets and glaciers at the end of Cenozoic. However, the question whether this increase is related to an increase in continental chemical weathering, or in mechanical weathering alone, is not clear.

Modelling: An Attempt to Integrate the Records into a Unified Framework

The Concept of Box Models

Biogeochemical cycles are usually described with box models. Such models provide a simple mathematical framework appropriate for calculating the geochemical evolution of the Earth through geological times. The Earth system is split into a relatively small number of components or reservoirs assumed to be homogeneous, such as the atmosphere, the ocean, the biosphere, the continental or oceanic crust, and the (upper) mantle. These reservoirs are connected by a series of 'arrows' representing the flows of material between them. The biogeochemical cycle of each element is thus represented as a set of interconnected reservoirs and, at any time, its state is characterized by the reservoir sizes or contents q_i (amount of the element in reservoir 'I', units: mol or kg) and the fluxes F_{ij} (amount of the element transferred per unit time from reservoir 'I' to reservoir 'j', units: mol y^{-1} or kg y^{-1}).

The temporal evolution of the system can be calculated by making a budget of input and output fluxes for each reservoir (eqn [2]).

$$\frac{\mathrm{d}q_i}{\mathrm{d}t} = \sum_{\substack{j=1 \\ j\neq i}}^{N} F_{ji} - \sum_{\substack{j=1 \\ j\neq i}}^{N} F_{ij} \qquad (i = 1, \ldots, N) \qquad [2]$$

To solve this system of differential equations, the values of the fluxes must be provided at each time step. Kinetic rate laws describing the dependence of the fluxes F_{ij} on the reservoir contents q_i, time t, or some external forcing are thus needed. Defining such kinetic rate laws is the most critical task of modeling. The reliability of the solution and hence the usefulness of the results depend strongly on the adopted rate laws. The challenge is clearly to get at least a first-order estimate of the fluxes from a very broad knowledge of the system, i.e., from the values of its state variables $q_1, \ldots, q_N$.

A useful concept in box modeling is that of turnover time. The turnover time of an element in a given reservoir is defined as the ratio between its reservoir content and its total output flux (eqn [3]).

$$\tau_i = \frac{q_i}{\sum_{\substack{j=1 \\ j\neq i}}^{N} F_{ij}} \qquad [3]$$

The turnover time can be seen as the time needed to empty the reservoir if the input happened to stop suddenly and the current output flux were held constant. It provides a first-order idea of the evolution timescale of a reservoir. At steady state (i.e., when input and output fluxes balance each other), the turnover time is equal to the residence time, which is the average time spent by individual atoms of the element in the reservoir. Finally, the response time of a reservoir characterizes the time needed for the reservoir to adjust to a new equilibrium after a perturbation.

Models of the Carbon Cycle

Figure 8 illustrates the present state of the long-term carbon cycle from a recent (unpublished) box model simulation of the authors. The reservoirs and fluxes that have been included in this figure are those that are important to describe the evolution of atmospheric CO_2 at the geological timescale. The values of reservoir sizes and fluxes are consistent with current knowledge of the system. Crustal reservoirs include continental (5000×10^{18} mol C) and pelagic (150×10^{18} mol C) carbonates, as well organic carbon (1250×10^{18} mol C) from the sedimentary cover. The atmosphere and ocean have been lumped into

one single reservoir containing 3.2×10^{18} mol C, since the time necessary for the atmosphere to reach equilibrium with the ocean is much shorter than ~ 1 My, the timescale of geological processes. Indeed, with a modern atmosphere-ocean exchange flux of 7.5×10^{15} mol C y^{-1} (i.e., 90 Gt C y^{-1}) and an atmospheric content of 62.5×10^{15} mol C (i.e., 750 Gt C), the turnover time of carbon in the atmosphere can be calculated to be only 8.33 years. Similarly, the terrestrial biosphere has not been included, since its size is small compared to other reservoirs and it can be assumed in equilibrium with the atmosphere–ocean system. The fluxes involved in the cycle are MOR/metamorphic CO_2 release ('volcanism'), weathering fluxes, and deposition of carbonates or organic carbon on the seafloor. The reported values of these fluxes are long-term averages, that is, they should be thought of as averages over several glacial–interglacial oscillations of the Pleistocene, although such averages cannot always be estimated from presently available data. The turnover time of carbon in the atmosphere–ocean reservoir in this 'geological' system can be calculated to be 143 000 y. Owing to this relatively short turnover time with respect to the timescale of long-term geological changes, the atmosphere–ocean system is essentially at equilibrium. By contrast, crustal reservoirs that exhibit much larger turnover times are not at equilibrium. This is clearly the case of continental ($\tau_i = 350$ My) and pelagic ($\tau_i = 50$ My) carbonate reservoirs, as a result of the Cenozoic deepening of the ocean lysocline and the associated transfer of carbonate deposition from the shelf to the pelagic environment.

To distribute the carbon content of the atmosphere–ocean system among its two components, and hence to derive the atmospheric P_{CO_2} value (and its effect on the climate), it is necessary to know the alkalinity content of the ocean. For this reason, the evolution of the ocean alkalinity (A_T) and ocean–atmosphere carbon (C_T) content are always calculated in parallel. Writing eqn [2] for these two variables yields eqns [4a] and [4b].

$$\frac{dA_T}{dt} = 2F_{SW} + 2F_{CW} - 2F_{CD} \qquad [4a]$$

$$\frac{dC_T}{dt} = F_{VOL} + F_{CW} - F_{CD} + F_{OW} - F_{OD} \qquad [4b]$$

F_{VOL} represents the total CO_2 release flux from volcanic origin (i.e., the sum of all metamorphic and MOR fluxes in **Figure 8**), F_{CW} and F_{SW} are the weathering fluxes from respectively carbonate and silicate rocks expressed in moles of divalent ions (Ca^{2+} or Mg^{2+}) per unit of time (i.e., the rates of reactions [I] and [II]), F_{CD} is the carbonate deposition flux, F_{OW} is the carbon input flux from weathering-oxidation of crustal organic carbon, and F_{OD} is the organic carbon deposition flux. Note that the silicate weathering flux does not appear in the carbon budget, eqn [4b], since silicate weathering (reaction [II]) transfers carbon from the atmosphere to the ocean but does not remove it from the atmosphere–ocean system. The factor of 2 in eqn [4a] results from the fact that two equivalents of alkalinity are transferred to the ocean when one Ca^{2+} or Mg^{2+} ion is delivered to the ocean by rivers (reactions [I] and [II]). The same factor of 2 holds for carbonate deposition, which is the reverse of reaction [I]. As already mentioned, the atmosphere–ocean system must be close to equilibrium, so that the derivatives on the left-hand side of eqn [4a] and [4b] can be set to zero. This assumption transforms the differential equation system into a set of two algebraic equations, which can be solved to yield eqn [5].

$$F_{VOL} - F_{SW} = F_{OD} - F_{OW} \qquad [5]$$

This equation leads to eqn [1] if the effect of the organic subcycle is neglected (i.e., when this subcycle is set to equilibrium). Hence, eqn [5] is a generalization of the Walker, Hays, and Kasting budget. It states that the disequilibrium of the inorganic part of the carbon cycle must be compensated for by a disequilibrium of opposite sign in the organic subcycle.

Use of Isotopic Data (Inverse Modeling)

To solve eqns [4] or [5], some kinetic laws must be provided for the fluxes, that is, the relations between these fluxes, time t, and the reservoir contents, or atmospheric P_{CO_2}, must be known. Such kinetic laws are, however, poorly known, so it may be preferable, at least for some fluxes, to use forcing functions in the calculation of these fluxes. For example, volcanic fluxes are often made proportional to the seafloor spreading rate and weathering fluxes to land area, for which past reconstructions are available. Ocean isotopic records, such as those presented earlier, can also be used to force the model. Budget equations similar to [2] are then written for the relevant isotopes and transformed into equations containing isotopic ratios r (or δ, the relative departure of the isotopic ratio from a standard). The sea water $^{87}Sr/^{86}Sr$ ratio has been used in this way to estimate the silicate weathering flux F_{SW}, but as discussed earlier the results are

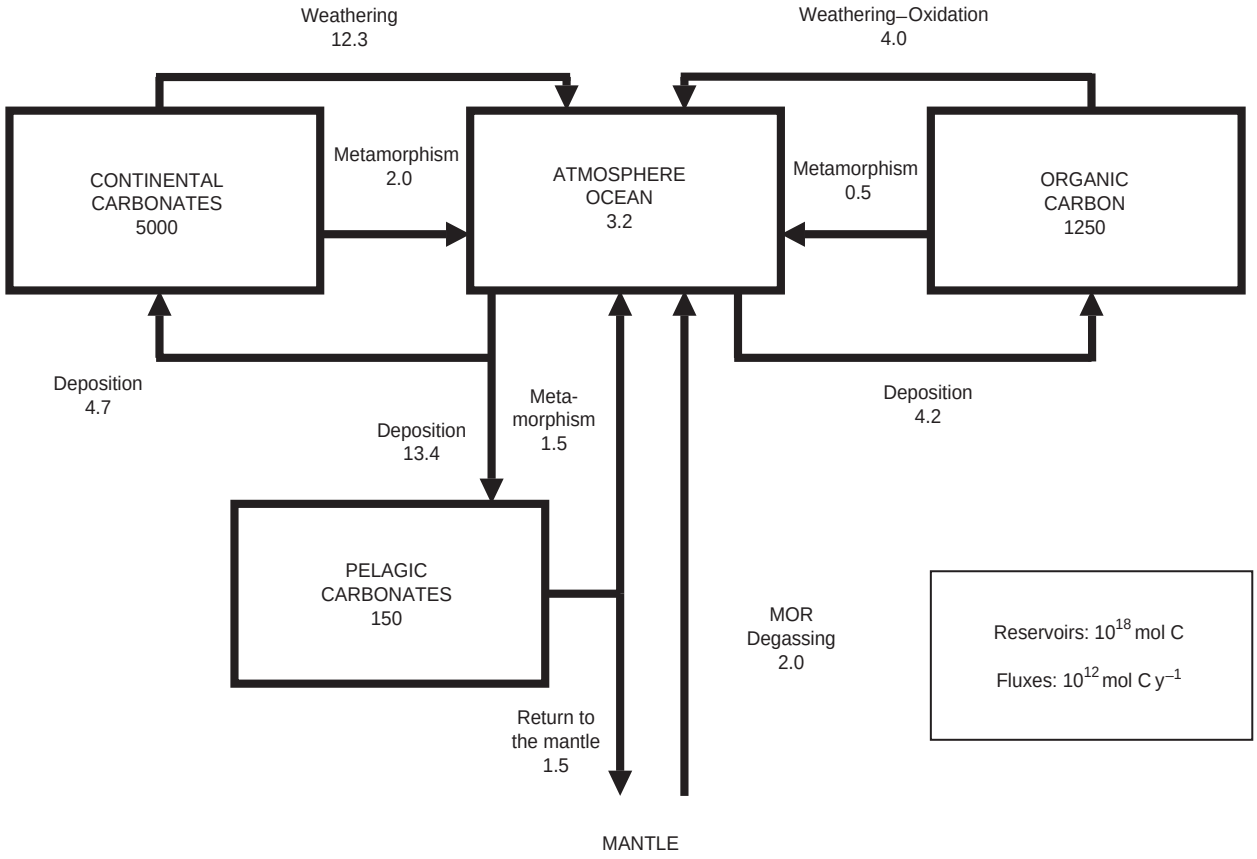

Figure 8 Present-day state of the long-term carbon cycle. Numbers represent 10^{18} mol C for reservoirs (boxes) and 10^{12} mol C y^{-1} for fluxes (arrows)

strongly dependent on the hypothesis of constancy for the isotopic ratios of weathered products. The ^{13}C isotopic history of the ocean has been used in many models, since the beginning of the 1980s, to constrain the organic carbon subcycle. The ^{13}C isotopic budget for the ocean can be written as eqn [6].

$$C_T\frac{d\delta_{oc}}{dt} = (\delta_{VOL} - \delta_{oc})F_{VOL} + (\delta_{CW} - \delta_{oc})F_{CW} + (\delta_{OW} - \delta_{oc})F_{OW} - (\delta_{OD} - \delta_{oc})F_{OD} \quad [6]$$

δ_{oc} here is the $\delta^{13}C$ of the ocean (more precisely, this should be the $\delta^{13}C$ of the atmosphere–ocean system); δ_{VOL}, δ_{CW}, and δ_{OW} are the $\delta^{13}C$ of the carbon inputs from respectively volcanic, carbonate weathering, and crustal organic carbon weathering–oxidation fluxes. It is assumed that no fractionation occurs with respect to average oceanic carbon during carbonate precipitation, so that this flux does not appear in the equation. $\delta_{OD} = \delta_{oc} - \Delta$ is the $\delta^{13}C$ of the organic carbon deposited on the seafloor, with Δ being the average fractionation of photosynthesis with respect to oceanic carbon (this includes both terrestrial and marine photosynthesis). The past values of δ_{oc} are known from the ^{13}C isotopic history of sea water (**Figure 5**). Equation [6] can then be solved with respect to F_{OD} and the resulting expression for F_{OD} is then used in eqn [4b] or [5]. The isotopic composition of the input fluxes must, however, be known or derived from similar isotopic budgets for the crustal reservoirs. This procedure is actually an inverse method, since it derives model parameters (fluxes) from an observed signal (ocean isotopic composition) linked to the model parameters through a mathematical operator (the isotopic budget equation). Y. Goddéris and L.M. François in 1996, and L.R. Kump and M.A. Arthur in 1997, published two separate models inverting the oceanic $\delta^{13}C$ signal over the Cenozoic, making use of an isotopic fractionation Δ variable with age and derived from paleodata. The Cenozoic histories

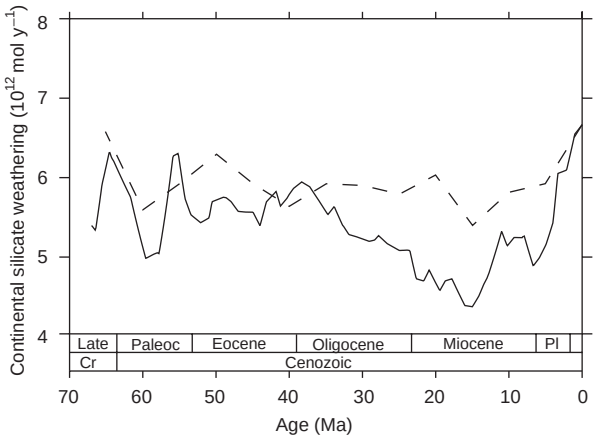

Figure 9 Model silicate weathering flux (solid line, Goddéris and François (1996); dashed line, Kump and Arthur (1997)). Timescale as **Figure 1**.

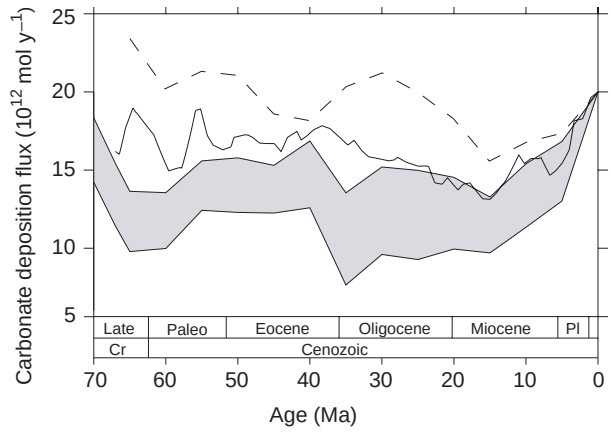

Figure 10 Model carbonate accumulation flux compared to the reconstruction of **Figure 4** normalized to the present day value of 20×10^{12} mol y^{-1} (solid line: Goddéris and François (1996); dashed line, Kump and Arthur (1997); shaded area, reconstruction from **Figure 4**.)

of silicate weathering from these models are compared in **Figure 9**. The predicted trend of the carbonate deposition flux is broadly consistent with an available reconstruction based on carbonate accumulation data (**Figure 10**).

A classical example of a box model using ^{13}C isotopic data to constrain the organic carbon subcycle is the BLAG model of Lasaga, Berner, and Garrels published in 1985. R.A. Berner in 1990 also used such an isotopic budget in GEOCARB to calculate the history of atmospheric CO_2 over the Phanerozoic. The results show a decreasing trend of atmospheric CO_2 over the Cenozoic. The trend is consistent with the overall trend reconstructed with other models (e.g., François and Walker, 1992) or from various paleoindicators (**Figure 1**). This does not mean, however, that we understand the carbon cycle (and climate) trends of the Cenozoic, since different models can produce similar trends from completely different underlying mechanisms. To be reliable, models should not rest only on a limited set of data but should be able to explain a wide range of geochemical records.

Conclusions

Proxy records indicate that the Earth's climate cooled gradually over the Cenozoic. This cooling trend was accompanied by a decrease of atmospheric P_{CO_2}. Other striking features of the Cenozoic are the sharp increase of the $^{87}Sr/^{86}Sr$ ratio of sea water and the overall deepening of the lysocline from late Eocene time to the present, and after the mid-Miocene a marked decrease of ocean $\delta^{13}C$ together with an increase in total carbonate accumulation and possibly phosphorus deposition. Are these environmental changes related? The role of models is to synthesize and provide a coherent explanation of such records, and then reconstruct the history of other key variables not directly accessible from paleodata. Today, we are still far from this goal. It is fundamental that models use multiple proxy data both as forcings and for validation, implying that other biogeochemical cycles for which proxies are available are modeled together with the carbon cycle. A coupling to other major biogeochemical cycles is also essential because of the interactions with the carbon cycle and the feedbacks involved.

See also

Calcium Carbonates. Carbon Cycle. Cenozoic Climate – Oxygen Isotope Evidence. Cenozoic Oceans – Carbon Cycle Models. Ocean Carbon System, Modelling of. Paleoceanography, Climate Models in. Past Climate From Corals. River Inputs. Sedimentary Record, Reconstruction of Productivity from the. Stable Carbon Isotope Variations in the Ocean.

Further Reading

Berner RA (1990) Atmospheric carbon dioxide levels over Phanerozoic time. *Science* 249: 1382–1386.

Berner RA (1998) The carbon cycle and CO_2 over Phanerozoic time: the role of land plants. *Philosophical Transactions of the Royal Society of London* B 353: 75–82.

Broecker WS and Peng TH (1982) *Tracers in the Sea*. Palisades: Eldigio Press.

Butcher SS, Charlson RJ, Orians GH and Wolfe GV (eds) (1992) *Global Biogeochemical Cycles*. London: Academic Press.

Chameides WL and Perdue EM (1997) *Biogeochemical Cycles: A Computer-Interactive Study of Earth System Science and Global Change*. Oxford: Oxford University Press.

Föllmi KB (1995) 160 My record of marine sedimentary phosphorus burial: coupling of climate and continental weathering under greenhouse and icehouse conditions. *Geology* 23: 859–862.

France-Lanord C and Derry LA (1997) Organic carbon burial forcing of the carbon cycle from Himalayan erosion. *Nature* 390: 65–67.

François LM and Walker JCG (1992) Modelling the Phanerozoic carbon cycle and climate: constraints from the $^{87}Sr/^{86}Sr$ isotopic ratio of sea water. *American Journal of Science* 292: 81–135.

Freeman KH and Hayes JM (1992) Fractionation of carbon isotopes by phytoplankton and estimates of ancient CO_2 levels. *Global Biogeochemical Cycles* 6: 185–198.

Goddéris Y and François LM (1996) Balancing the Cenozoic carbon and alkalinity cycles: constraints from isotopic records. *Geophysical Research Letters* 23: 3743–3746.

Harland WB, Armstrong RL, Cox AV, *et al.* (1990) *A Geologic Time Scale 1989*. Cambridge: Cambridge University Press.

Hayes JM, Strauss H and Kaufman AJ (1999) The abundance of ^{13}C in marine organic matter and isotopic fractionation in the global biogeochemical cycle of carbon during the past 800 Ma. *Chemical Geology* 161: 103–125.

Kump LR and Arthur MA (1997) Global chemical erosion during the Cenozoic: weatherability balances the budgets. In: Ruddiman WF (ed.) *Tectonic Uplift and Climate Change*. New York: Plenum Press.

Kump LR, Kasting JF and Crane RG (1999) *The Earth System*. New Jersey: Prentice Hall.

Lasaga AC, Berner RA and Garrels RM (1985) An improved geochemical model of atmospheric CO_2 fluctuations over the past 100 million years. In: Sundquist E and Broecker WS (eds) *The Carbon Cycle and Atmospheric CO_2: Natural Variations Archean to Present* Geophysical Monograph 32, pp. 397–411. Washington, DC: American Geophysical Union.

Opdyke BN and Wilkinson BH (1988) Sea surface area control of shallow cratonic to deep marine carbonate accumulation. *Paleoceanography* 3: 685–703.

Pearson PN and Palmer MR (2000) Atmospheric carbon dioxide concentrations over the past 60 million years. *Nature* 406: 695–699.

Raymo ME (1991) Geochemical evidence supporting T.C. Chamberlin's theory of glaciation. *Geology* 19: 344–347.

Ruddiman WF (ed.) (1997) *Tectonic Uplift and Climate Change*. New York: Plenum Press.

Van Andel TH (1975) Mesozoic-Cenozoic calcite compensation depth and the global distribution of calcareous sediments. *Earth and Planetary Science Letters* 26: 187–194.

Van Andel TH (1994) *New Views on an Old Planet: a History of Global Change*, 2nd edn. Cambridge: Cambridge University Press.

Walker JCG, Hays PB and Kasting JF (1981) A negative feedback mechanism for the long-term stabilization of Earth's surface temperature. *Journal of Geophysical Research* 86: 9776–9782.

CEPHALOPODS

P. Boyle, University of Aberdeen, Aberdeen, UK

doi:10.1006/rwos.2001.0195

Introduction

The Cephalopoda is the class of the Mollusca comprising the octopuses, cuttlefish, squid, and their allies. Exclusively marine and present in all of the world's oceans and seas, their lineage can be traced from the Ordovician to the present due to fossilization of their large, heavy, chambered shells. The Pearly Nautilus (*Nautilus* spp.) of the Indo-Pacific region is the only surviving relative of this ancient ancestry (10–12 000 extinct species) Modern living cephalopods (subclass Coleoidea), having reduced or lost the ancestral shell, are represented by only about 650–700 species. These are characteristically large, active, soft-bodied predators, with complex behavioral and physiological capabilities. Occupying a wide range of benthic and pelagic habitats they are abundant in productive shelf regions, where genera such as *Octopus* and the common cuttlefish *Sepia* are each credited with over 100 species. The greatest diversity of form and biomass of cephalopods is oceanic and mesopelagic in distribution, but the biology of these offshore species is little understood and generalizations are based mostly on coastal forms. Now, and throughout their evolutionary history, representatives of the cephalopods reach the largest of all invertebrate body sizes.

With the exception of *Nautilus* (and some of the deep-sea forms), cephalopods generally share